Tikrit Journal of Engineering Sciences (2025); 32(1): 1469
DOI: http://doi.org/10.25130/tjes.32.1.33

IRAQI Academic Scientific Journals

ISSN: 1813-162X (Print); 2312-7589 (Online)

Tikrit Journal of Engineering Sciences

available online at: http://www.tj-es.com

TJES Tikrit Journal of Engineering Sciences

Performance Enhancement of Phase Change Material PCM Thermal Energy Storage TES System Using Nanoparticles Additives: An Experimental Investigation

Ebtehal S. Hussain *, Ihsan Y. Hussain
Mechanical Department, Engineering College, Baghdad University, Baghdad, Iraq.

Keywords:
Discharging Process; Nanoparticles; Paraffine Wax; Stability of Nanoparticles; Thermal Cycle Effect; Thermal Energy Storage.

Highlights:

- *The improvement in thermal distributions of paraffin mixed with 0.5% Tio2 was better than paraffin mixed with 0.5% gamma and 0.5% alpha at 1 m/s HTF velocity.*
- *Repeating the thermal cycle negatively affected the PCM thermal behavior of the paraffine wax test with 0.5% alpha and 0.5% gamma at a velocity of 3 m/s.*
- *The largest improvement of thermal conductivity of nano-PCM compared to pure wax was 56.80% at 1% Tio2.*

ARTICLE INFO

Article history:

Received	03 Aug. 2023
Received in revised form	03 Nov. 2023
Accepted	15 Nov. 2023
Final Proofreading	31 Mar. 2024
Available online	28 June 2025

Citation: Hussain ES, Hussain IY. **Performance Enhancement of Phase Change Material PCM Thermal Energy Storage TES System Using Nanoparticles Additives: An Experimental Investigation**. *Tikrit Journal of Engineering Sciences* 2025; **32**(1): 1469.
http://doi.org/10.25130/tjes.32.1.33

**Corresponding author:*

Ebtehal S. Hussain
Mechanical Department, Engineering College, Baghdad University, Baghdad, Iraq.

Abstract: Paraffin wax used as Phase Change Material (PCM) in Thermal Energy Storage (TES) is one possible solution to store excess energy as heat and release it when power generation is insufficient. However, the PCM had a disadvantage: low thermal conductivity. So, the researchers developed some methods for increasing it since PCM is critical for a wide range of technologies. The present study describes experimentally the investigation of the discharging process of paraffin wax dispersed with different concentrations (0.5% and 1%) of gamma-alumina oxide (39.2 nm), titanium oxide (47.2 nm), and alpha-aluminum oxide (186 nm), in TES system for different heat transfer fluid (HTF) velocities, i.e., 1 m/s, 3 m/s, and 5 m/s. The influence of nanoparticles on the PCM thermo-physical properties. The effect of discharging cycles on the stability of nanoparticles was also investigated. The findings indicated that the improvement in thermal distributions of paraffin mixed with 0.5% TiO_2 was better than paraffin mixed with 0.5% gamma and 0.5% alpha at 1 m/s HTF velocity, while at 1% concentration, the gamma alumina was more effective than others in modifying the paraffine wax thermal behavior since the time-saving of it was 19.54% compared to pure paraffine. Repeating the thermal cycle negatively affected the PCM thermal behavior of the paraffine wax test with 0.5% alpha and 0.5% gamma at a velocity of 3 m/s. However, a relative enhancement of nearly 7.69% in solidification time for 0.5% Tio2 was found. At the same velocity (3 m/s), the reduction in solidification time of gamma alumina and Tio2 was 12.3% and 7.69%, respectively, with a mass fraction of 1%. The largest improvement of thermal conductivity of nano-PCM compared to pure wax was 56.80% at 1% TiO_2. Furthermore, the improvement in heat transfer rate at 0.5% Tio2 and 1% gamma was 15.67% and 68.64%, respectively. The "negative" results of repeated thermal cycles indicated that the stability of nano-PCM remains a big challenge and requires a multidisciplinary approach to determine the behavior of nanomaterials in a dispersing medium.

تحسين الاداء لمنظومة خزن الطاقة الحرارية لمادة متغيرة الطور باستخدام اضافة الجسيمات النانوية: دراسة عملية

إحسان يحيى حسين، ابتهال سلمان حسين
قسم الهندسة الميكانيكية / كلية الهندسة / جامعة بغداد / بغداد – العراق.

الخلاصة

شمع البارافين المستخدم كمواد متغيرة الطور (PCM) في مخازن الطاقة الحرارية (TES) هو أحد الحلول الممكنة لتخزين الطاقة الزائدة على شكل حرارة وإطلاقها عندما يكون توليد الطاقة غير كافٍ. ومع ذلك ، كان لـ PCM عيبًا ، وهو الموصلية الحرارية المنخفضة. لذلك طور الباحثون بعض الطرق لزيادتها لأن PCM أمر بالغ الأهمية لمجموعة واسعة من التقنيات. تصف الدراسة الحالية بشكل تجريبي التحقيق في عملية تفريغ شمع البارافين المشتت بتركيزات مختلفة (٠,٥٪ و ١٪) من أكسيد جاما الألومينا (٣٩,٢ نانومتر) وأكسيد التيتانيوم (٤٧,٢ نانومتر) وأكسيد الألومنيوم ألفا (١٨٦ نانومتر). ، في نظام (TES) وعند سرعات مختلفة لمائع انتقال الحرارة وهي هي (١ م/ث)، (٣ م/ث)، (٥ م/ث)، كما تم دراسة تأثير الجسيمات النانوية على الخواص الفيزيائية الحرارية للـ PCM وتأثير دورات التفريغ على ثبات الجسيمات النانوية. تشير النتائج إلى أن التحسن في التوزيعات الحرارية للبارافين الممزوج بـ (٠,٥٪ Tio2)كان أفضل من البارافين الممزوج بـ (٠,٥٪ جاما) و (٠,٥٪ ألفا) بسرعة (١ م / ث) لل(HTF) ، بينما عند (تركيز ١٪) كان gamma alumina أكثر فاعلية من غيره في تعديل السلوك الحراري لشمع البارافين حيث كانت نسبة التحسن لوقت التفريغ (١٩,٥٤٪) مقارنة بالبارافين النقي. أثر تكرار الدورة الحرارية سلبًا على السلوك الحراري PCM لاختبار شمع البارافين بنسبة ٠,٥٪ ألفا و٠,٥٪ جاما عند السرعة (٣ م/ث)، ولكن تحسن نسبي يقارب ٧,٦٩٪ في وقت التصلب لـ ٠,٥٪ Tio2. وبنفس السرعة (٣ م/ث)، يبلغ الانخفاض في وقت التصلب لألومينا جاما وTio2 (12.3% و٧,٦٩٪) على التوالي، مع نسبة كتلة تبلغ ١٪. أكبر تحسن في التوصيل الحراري للnano-PCM مقارنة بالشمع النقي كان (٥٦,٨٠٪) عند ١٪ TiO_2. علاوة على ذلك ، فإن التحسن في معدل انتقال الحرارة عند (٠,٥٪ TiO_2 ، و ١٪ gamma) بلغ (١٥,٦٧٪ ، ٦٨,٦٤٪) على التوالي. تشير النتائج "السلبية" للدورات الحرارية المتكررة إلى أن استقرار nano-PCM لا يزال يمثل تحديًا كبيرًا ويتطلب نهجًا متعدد التخصصات لتحديد سلوك المواد النانوية في وسط التشتت.

الكلمات الدالة: عملية التفريغ، الجسيمات النانوية، شمع البارافين، استقرار الجسيمات النانوية، تأثير الدورة الحرارية، مخازن الطاقة الحرارية.

1.INTRODUCTION

Renewable energy sources, like hydrogen fuel cells and other renewable energies like solar, wind, and nuclear power, may become viable alternatives to fossil fuels [1]. So renewable energy sources are very important to meet the rising demand for energy while simultaneously controlling environmental pollution. Thermal Energy Storage (TES) is one possible solution for storing excess energy as heat and releasing it when power generation is insufficient [2]. Usually, thermal energy can be stored in various forms, such as latent heat storage, sensible heat storage, and thermochemical heat storage [3]. The energy in a thermal energy storage system can be stored using base materials such as Phase-Change Material (PCM) that can release and absorb thermal energy [4]. The most promising material is paraffin wax due to its desirable properties, such as low melting pressure, high chemical stability, no supercooling, 100% recyclable, and considerable latent heat of fusion [5]. However, they require more time to store and release energy due to their low thermal conductivity. So, the researchers developed some methods to increase it [6]. Extended surface/fins inside the PCM domain and nanomaterial additives significantly influence PCM thermal conductivity in the Latent Heat Storage (LHS) system [7]. Nanotechnology has emerged as one of the most significant and attractive frontier fields in Physics, Chemistry, Engineering, and Biology. It offers several breakthroughs in the near future that will change the direction of technical developments in a wide range of applications; for example, adding nanoparticles to diesel fuel enhances engine performance by reducing greenhouse gas emissions and reducing fossil fuel pollutants and their environmental effects [8]. Also, control the flow of the heat through the roof of the building exposed to a high amount of thermal load using nanomaterials; since nanomaterials have high properties, this made them good elements of the energy conservation strategy in the architectural field [9]. The most common type of solar collector used to collect solar energy is a flat-plate solar collector (FPSC). Its thermal performance can be improved using heat transfer fluid dispersions with particles in the range of nanosized particles, such as multi-walled carbon nanotubes [10]. Also, the wind turbines can be improved using nanoparticles, which increase wind turbines' resistance to fatigue, wear, failure, and tough operating conditions [11]. The new class of material can be obtained by adding nanoparticles in the PCM, called "nano-PCM," which is used in different applications, such as enhancing the thermal properties of paraffin wax. Several studies have been conducted on using nano-PCM, a new class of materials in a wide range of techniques. Arasu et al. [12] studied theoretically the effect of the nanoparticle concentration on the melting-solidification process of PCM distributed with (0%, 1%, 3%, and 5%) of copper oxide (CuO) and alumina (Al_2O_3). The results showed that nanoPCM melted faster (4.8% and 2.9%) for 1% alumina and copper oxide, respectively, than pure paraffin wax. Buonomo et al. [4] numerically studied the influence of adding metal foam and nanoparticles into PCM on the Latent Heat Thermal Energy System (LHTES). The volume content of alumina (Al_2O_3) was 1%. The obtained results revealed that the charging time for pure PCM, nano-PCM, and nano-PCM with metal foam was (40301, 39781, and 1321 sec), respectively. Mahdi and Nsofor [13] numerically studied the impact of using Al_2O_3 nanoparticles with (3%, 5%, and 8%) concentrations on the solidification process of PCM in triplex-tube TES. The results showed that dispersing alumina nanoparticles of 3% to 8 % of volumetric concentrations reduced the total discharge time by 8% and 20%, respectively. Chaichan et al. experimentally [14] studied the paraffin wax's thermal conductivity improvement with (1%, 2%, 3%, 4%, and 5%) mass fractions of alumina (Al_2O_3) and (TiO_2) during the discharging and charging process. The findings indicated that charging time decreased from about 13 to 5 minutes when 5% nano-Al2O3 was added, while it was reduced from 13 to 7 minutes with 5% nano-TiO2. A 5% mass fraction of nano-Al2O3 reduced the discharging time from 22 to 11 minutes, while it was reduced from 22 to 13 min with 5% nano-TiO2. Pradeep et al. [15] conducted an experimental investigation on the impact of adding 0.05% and 0.1% of silver nanoparticles on paraffin wax's melting/solidification characteristics. The experimental setup consisted of a concentric pipe. PCM was stored in the annular area between the inner and outer pipes. The results showed that adding very small amounts of silver nanoparticles reduced the charging/discharging temperatures of paraffin wax by (10.8% and 27.9%) for concentrations of (0.05% and 0.1%), respectively, during the melting process and by (11% and 29.5%) for (0.05% and 0.1%) concentrations, respectively, during the solidification process. Teng and Yu [16] added silica, alumina, titania, and zinc oxide to paraffin wax at different concentrations (1%, 2%, and 3%) to investigate the impacts of different nano-additives concentrations on the performance of heat conduction and thermal energy storage. The experimental results showed that the ratio of Melting Onset Temperature (T_{mo}) decreased by (0.91%, 0.72%, and 0.54%) by adding (1%, 2%, 3%) mass fraction of nano-Al2O3, respectively, and by (1.33%, 1.13%, and 0.85%) by adding (1%, 2%, and 3%) mass fraction of TiO2, respectively. The maximum enhanced ratio of Solidification Onest Temperature (T_{SO}) was 1.8% by adding 2% concentrations of ZnO. Adding TiO2 reduced paraffin's phase-change heat by less than 0.46% for Melting Heat (H_m) and Solidification Heat (H_s). Venkateshwar et al. [17] experimentally investigated the different potential techniques to quantify the concentration of nanoparticles after each thermal cycle of PCM; the nanoparticles concentrations used in this study were (0.5% wt. and 1% wt.) of Fe_3O_4 and CuO in coconut oil and Rubither35 HC. The results of the experimental study indicated that higher concentration nano-PCM exhibited more pronounced sedimentation, thermal cycling caused higher Fe_3O_4 nanoparticle sedimentation than Cuo, and after two thermal cycles, the concentration of Fe_3O_4 decreased from (1% wt. to 5.69×10^{-6} %, and from 0.5% wt. to 8.93×10^{-6} %), while the concentration of CuO decreased from (1% wt. to 1.34×10^{-5}, and from 0.5% wt. to 1.72×10^{-5}). Li et al. [18] experimentally investigated the effect of adding (0.01%, 0.1%, and 1%) volume fraction of Al_2O_3 nanoparticles into paraffin wax on its thermophysical properties. The results showed that the thermal conductivity of three nanoPCMs improved at 20°C compared to pure paraffin wax, with a volume fraction of 0.01% showing the greatest improvement (40%) in thermal conductivity. In the solid state, the thermal diffusivity of nanofluids with volume fractions of 0.01%, 0.1%, and 1% varied by (-31%, 13.5%, and -21%), respectively. With a temperature rise, the Volumetric Heat Capacity (VHC) changed. For volume fractions of 0.01% and 0.1%, VHC was larger than 1% in the liquid form. Hiba and Ihsan [19] investigated the performance enhancement of CTESS experimentally using metal foam. The results demonstrated that the average Nusselt number and the total thermal power of heat transfer fluid at ambient temperature were about (24.25% to 42.03%) and (16.82% to 35.23%), respectively. In their study, [20] Sadiq and Mussa determined how thermal conductivity affected thermal energy performance when solidifying two paraffin wax types with different thermal conductivities. The results showed that PCM's efficiency in Case 2 with (0.3 W/m K) increased by 13.15% compared to Case 1 with (0.265 W/m K). Abdulateef et al. [21] numerically and experimentally studied the effect of alumina nanoparticles' added (5% and 10% concentrations) in the triplex-tube heat exchanger. The results showed that compared with fins without nanoparticles, fins-nanoparticle enhanced the solidification time by 33% and 34% for internal longitudinal fins-nanoparticle and internal triangular fins-nanoparticle, respectively. Khalaf et al. [22] experimentally investigated the effect of different variables, such as Rayleigh number, Taylor number, Richardson Number, and nanoparticle volume fractions (φ) of Al_2O_3 with water base ($0\ \% \le \varphi \le 0.225\ \%$) on the heat transfer augmentation for Taylor-Couette flows between concentric cylinders. The results showed that the enhancement in heat transfer was 16.5% to 24% due to rising the Al2O3-pure water concentration from 0% to 0.225%. Several researchers conducted experimental and theoretical investigations to improve the thermal characteristics of PCM. As concluded from the literature review, high-conductivity nanomaterial additions can effectively improve PCM thermal conductivity and enhance the thermal performance of LHS systems. However, the type, concentrations, repeated thermal cycles, and dispersion of nanomaterial in PCMs directly affect the thermal performance of PCMs. The present study experimentally analyzed the improvement in temperature distributions and the changes in the thermophysical properties of paraffin wax caused by nanoparticle dispersion. Discharging processes were studied for paraffine wax with and without adding nanoparticles in different concentrations. The effect of repeated thermal cycles on the stability of nanoparticles within PCM was also studied.

2.EXPERIMENTAL PROGRAM SETUP

2.1.Experimental Setup

Figures 1 and 2 illustrate the experimental system's schematic diagram and test rig, respectively. The experimental system mainly consisted of a blower and four sections: the transient, entrance, test, and exit. A transition section connected the blower and entrance section. The test section consisted of three boxes; one of them was used for placing PCM with internal dimensions (400mm × 100mm × 20mm) (L×W×H). The heat transfer fluid (HTF) was the air at ambient temperature that passed through the PCM top and bottom. HTF exchanged heat with PCM along its flow path at different velocities, i.e., 1, 3, and 5 m/s. The two air sides are HTF sides with dimensions (100 mm×25 mm) (W×H). The base of the box was made of a copper plate with a thickness of 1.5 mm, and its sides were made of Perspex. Also, the surface between the lower and upper HTF sides used a copper plate with a 1.5 mm thickness. Variac (type TDGC 2-3KVA and input = 220W, output = 0 – 250 V, and Capacity = 3000 VA) was connected to a blower centrifugal type rotates 6500 rpm with 230V and 220W to control the input voltage to get the required velocity. A hot wire anemometer (model: YK-2005AH, Lutron electronic enterprise company with accuracy ±0.001 m/s) was used to measure the velocity values at the test section's entrance. To measure the distribution of transient temperature of PCM and HTF sides, K-type thermocouples (Chromel alloy Nickel-Chromium, with accuracy 0.75%) with 0.5 mm diameter were used. Three of them were embedded through the center of the PCM, and another one was fixed on the box base of the PCM. For each air passage, three thermocouples were used; two of them were fixed at the entrance and exit of the test section, and another one was fixed opposite the center of the PCM box and attached to the copper plate, which separated between the box and the upper and lower air passages, as shown in Fig. 1. Accordingly, the total number of thermocouples in the upper and lower air passages were six thermocouples. The thermocouples were connected to a data logger (model: AT45 32 Multi-channel Temperature Meter, Applent Instruments company with accuracy ±0.5 ^{o}C) to measure the temperature and save it on an SD memory card.

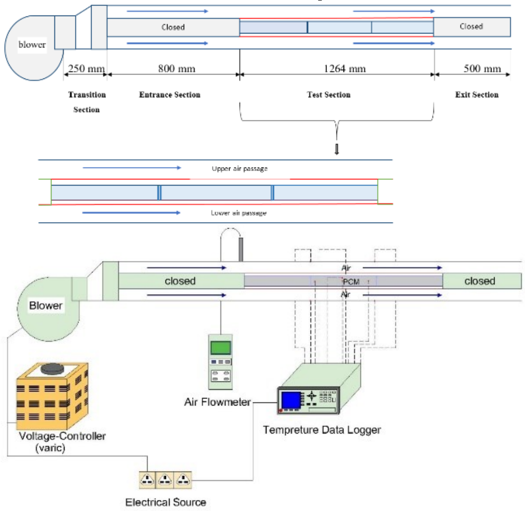

Fig. 1 Schematic Sketch and Dimensions of Experimental System, All Dimensions in (mm).

(a) Test Rig.

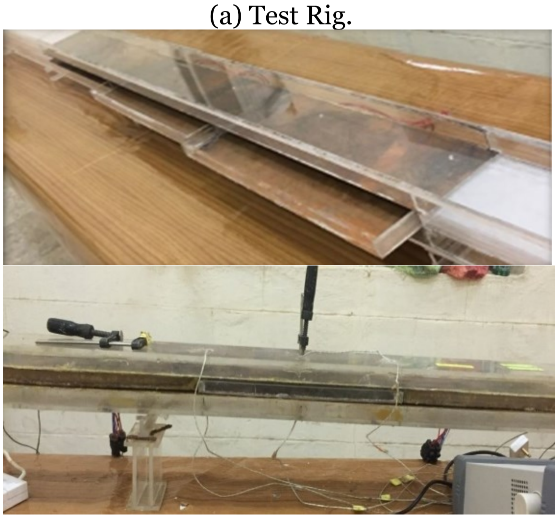

(b) Test Section.

Fig. 2 Experimental System's Test Rig and Test Section.

2.1.1.Materials

Materials used in the present work are:

1) Phase Change Materials (PCMs): the type of PCM used in the present work was paraffin wax, which was from the Al-

Daura refinery (Iraq). Various properties of these nanoparticles, measured at the Science and Technology Laboratory, are presented in Table 1.

2) Nanoparticles: For the present study, gamma-aluminum oxide (39.2 nm), titanium oxide (47.2 nm), and alpha-aluminum oxide (186 nm) nanoparticles were purchased from (US Research Nanomaterials, Inc., USA). An Atomic Force Microscope (AFM) (AaioAFM 2022, Nanosurf AG Switzerland) was used to determine the mean particle size of nanoparticles, as shown in Fig. 3. Various properties of these nanoparticles are presented in Table 2.

Table 1 Thermophysical Properties of PCM.

Properties	Paraffin Wax
Melting Temperature [K]	339.5
Solidus Density [kg/m^3]	852.14
Liquidus Density[kg/m^3]	766.11
Specific Heat [J/kg K]	2900
Thermal Conductivity [W/m K]	0.4
Dynamic Viscosity [kg/m s]	0.027
Latent Heat [J/kg]	270715

Table 2 Thermal Properties of Nanoparticles Used.

Properties	Nanoparticles Used		
	Al_2O_3		Tio2
	Alpha	Gamma	
Purity	99.9%	99.9%	99.9%
Color	white	white	white
Mean Diameter (nm)	186.2	39.2	47.2
Thermal Conductivity[W/m K]	36	36	8

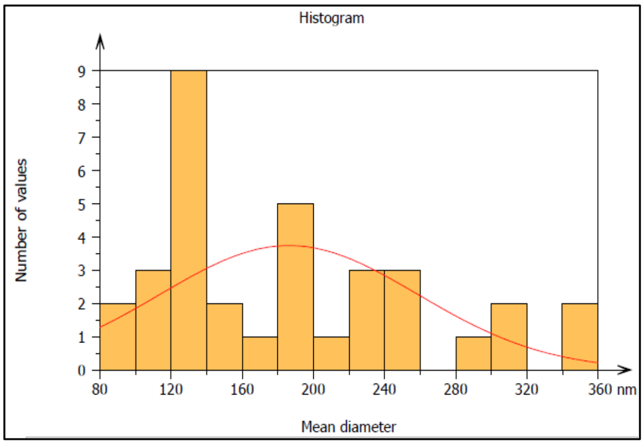

(a) Alpha Mean Diameter.

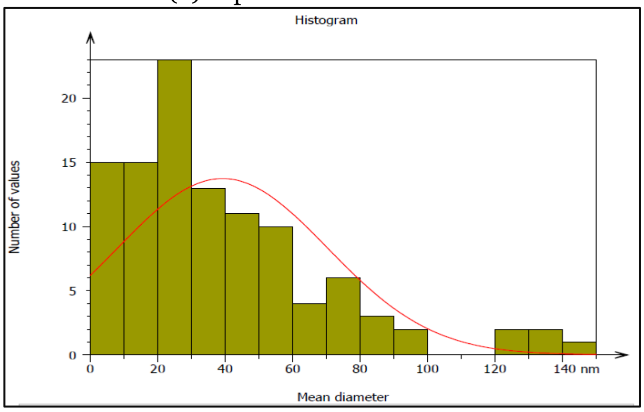

(b) Gamma Mean Diameter.

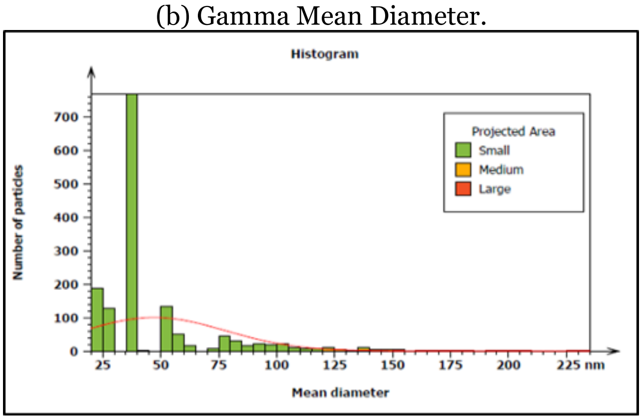

(c) Tio2 Mean Diameter.

Fig. 3 The Mean Particle Size of Nanoparticles.

2.2. Preparation of PCM-Nanoparticle Mixture

2.2.1. Nano Dispersion with PCM

There is no standardized method to prepare the nano-PCM. Previous studies used mechanical and chemical methods to mix nanoparticles with PCM. Sonication and stirring are two types of mechanical dispersion. Stirring the magnetic bar in the liquid medium helps nanoparticles diffuse at a larger scale. In contrast, sonication was used to provide good dispersion since the collapse of microbubbles resulting from this process leads to the disentanglement of clustered and agglomerated nanoparticles. For preparing the nano-PCM, the following steps were followed, as shown in Fig. 4:

1) The nanoparticle and paraffin wax were separately weighted using an electronic balance (measuring range 0 – 200 g, precision 0.1 mg).
2) The paraffine wax was initially heated on a hot plate to a temperature above its melting point.
3) The required mass fraction of nanoparticles was added to the liquid paraffin wax gradually and slowly. Then, the mixture was stirred over a magnetic stirrer for at least 2 hours by setting the mixture temperature (75-80) °C, which is higher than the melting point of nano-PCM. The mixture was placed under sonication for another 2 hours to obtain a homogenous mixture.

(a) The nanoparticle and PCM were Weighted by an Electronic Balance.

(b) Hot Plate Magnetic Stirrer with Water Path Sonication.

Fig. 4 Nano Dispersion with PCM.

The compositions of samples prepared with different concentrations of nanoparticles with paraffin wax are presented in Table 3. The quantities of nanoparticles were determined by the weight method. In this method, the nanoparticles concentration was calculated using the following equation [23]:

$$\emptyset = \frac{m_{np}}{m_{np} + m_{pcm}} \quad (1)$$

where Ø%, m_{np}, and, m_{pcm} are the nanoparticles concentration, nanoparticles mass (kg), and PCM mass (kg), respectively. In the recent study, gamma-alumina (Al_2O_3), titanium oxide (Tio_2) nanoparticles, and alpha-alumina particles were added into Iraqi paraffine wax with (0.5% and 1%) concentrations to evaluate the effect of nanoparticles on the PCM thermal behavior. The thermal conductivities of PCM and Nano-PCM were examined using Lee's Disc method, as in reference [20]. The BROOKFILLD device (Model RVDV-I Prime, Voltage 230 V~, Frequency 50/60 Hz, and Power 22 Watts) was used to measure the viscosity of the PCM and Nano-PCM. It has a spindle that rotates at a speed of 100 rpm. To measure the viscosity, the spindle must have been immersed in a 150 ml beaker filled with the sample in a liquid state.

Table 3 Composition of Prepared PCM/NanoPCM Sample.

Sample Name	Composition of Samples (in gram)
Pure Paraffine	682 Paraffin Wax
Paraffine+0.5% Alpha	678.5 Paraffine Wax+ 3.4 Alpha-Alumina
Paraffine+ 1% Alpha	675 Paraffine Wax+ 7 Alpha-Alumina
Paraffine+ 0.5% Gamma	678.5 Paraffine Wax+ 3.4 Gamma-Alumina
Paraffine+ 1% Gamma	675 Paraffine Wax+ 7 Gamma-Alumina
Paraffine+ 0.5% Tio_2	678.5 Paraffine Wax+ 3.4 Tio_2
Paraffine+1% Tio_2	675 Paraffine Wax+ 7 Tio_2

2.3.Experimental Procedure and Data Reduction

The experimental investigation of the discharge process for a single thermal energy storage system was conducted, and the following procedure was followed: Preparation of PCM-nanoparticle mixture as explained previously. Molten PCM was poured into the middle box of the test section. Waited a while to ensure that the average temperature of PCM reached about 70 °C. The blower with a specific speed was turned on. Then, the temperature distribution of PCM was recorded by the data acquisition (data logger) at every second and recorded on the SD. The process ended when the temperature of paraffin wax reached about 50 °C. The procedure above was repeated with the remaining velocities. The necessary variables for the heat transfer process were located using the typical heat exchanger correlation that [24] described. The bulk mean temperature (T_b) was used to find the thermophysical properties of air,

$$T_b = \frac{T_{in} + T_{out}}{2} \quad (2)$$

where T_{in} is the inlet air temperature, and T_{out} is the outlet air temperature. The rate of convection heat transfer (also called thermal power (Q)) between the hot PCM and cold air was calculated by Newton's law of cooling.

$$Q = h_a A_s LMTD \quad (3)$$

where A_S and h_a are the surface area of the copper plate between the PCMs and the air and the convective heat transfer coefficient of HTF, respectively, and LMTD is the log-mean temperature difference between PCM and air [25].

$$LMTD = \frac{(T_s - T_{in}) - (T_s - T_{out})}{\ln\left(\frac{T_s - T_{in}}{T_s - T_{out}}\right)} \quad (4)$$

where T_S is the temperature of the copper plate between the PCMs and the air. According to the energy balance, when losses are ignored, the energy increase of the side of the air channel equals the heat transfer rate between the PCM and the air.

$$Q = \dot{m}\, C_p\, (T_{out} - T_{in}) = h_a\, A_s\, LMTD \quad (5)$$

The convective heat transfer coefficient (h_a) value is calculated using the above equation.

$$h_a = \frac{Q}{A_s\, LMTD} \quad (6)$$

$$\dot{m} = \rho\, V\, A_c \quad (7)$$

where $\dot{m}$, C_p, and V are the air mass flow rate, density, specific heat, and velocity, respectively. A_c is the cross-section area of the air passage side. The Nusselt Number (Nu) was calculated after calculating the heat transfer coefficient (h_a) by applying the flowing equations.

$$Nu = \frac{h_a D_h}{K_a} \quad (8)$$

$$D_h = \frac{4 A_c}{p} \quad (9)$$

where K_a is the thermal conductivity of air, D_h is hydraulic diameter, and p is the perimeter. Eqs. (5) and (8) were applied at the box's upper and lower air passages to find the thermal power and the Nusselt number.

3.EXPERIMENTAL UNCERTAINTY

Uncertainty analysis was used to evaluate the propagation of error in heat transfer rate. The suggested method by Holman [26], was used to evaluate the uncertainty estimate. The uncertainty is given by:

$$\delta R = \frac{\partial R}{\partial V_1} \delta V_1 + \frac{\partial R}{\partial V_2} \delta V_2 + \cdots + \frac{\partial R}{\partial V_n} \delta V_n \quad (10)$$

$$W_R = \left[\left(\frac{\partial R}{\partial V_1} W_1\right)^2 + \left(\frac{\partial R}{\partial V_2} W_2\right)^2 + \left(\frac{\partial R}{\partial V_n} W_n\right)^2 \right]^{0.5} \quad (11)$$

where $V_1, V_2, and\ V_n$ are independent variables of defined results, and W_R is the parameter's uncertainties. The heat transfer rate is a function of several variables.

$$Q = f\,(v\,, \Delta T, A_c) \quad (12)$$

Due to errors made by device manufacturers, some parameters were measured directly. An uncertainty number can be assumed, such as the thermocouple accuracy used to measure temperature was (0.04 °C), the airflow meter accuracy was (±0.001 m/s), and the length had errors was (±0.0002 m). The experimental error in the heat transfer rate calculation can be expressed as follows:

$$\frac{W_Q}{Q} = \left[\left(\frac{\partial Q}{\partial V} \cdot \frac{W_v}{Q}\right)^2 + \left(\frac{\partial Q}{\partial \Delta T} \cdot \frac{W_{\Delta T}}{Q}\right)^2 + \left(\frac{\partial Q}{\partial A_c} \cdot \frac{W_{A_c}}{\partial A_c}\right)^2 \right]^{0.5} \quad (13)$$

So, the uncertainty of the heat transfer rate was 8.03%.

4.RESULTS AND DISCUSSION

4.1.The Effect of Nanoparticles on Thermal Behavior of PCM

Two different concentrations of alpha alumina, gamma alumina, and TiO_2 nanoparticles in paraffine wax were studied. Different velocities were considered and the temperature behaviors of nano PCM and pure PCM were performed. Figures 5 and 6 show the PCM temperature distribution at (1 m/s) and two mass fractions (0.5% and 1%), respectively. The results showed that the additives of nanoparticles improved the thermal distributions of the paraffin wax since dispersing nanoparticles increased the thermal conductivity of the PCM, resulting in greater heat transfer from the PCM to the heat transfer fluid, thus increasing the amount of heat transferred through the wax. Figure 5 indicates that paraffin mixed with (0.5% Tio_2) is better than paraffin mixed with (0.5% gamma) and (0.5% alpha) at the same HTF velocity since the time taken by pure wax and nanoPCM with 0.5% Tio2, gamma-alumina, and alpha-alumina for complete solidification was (87, 75, 85, and 87 min), respectively. At (1% concentration), the solidification time for gamma alumina and alpha-alumina to reach 50 ^oC was the same. The time-saving of nanoPCM with Tio_2 and gamma alumina was determined to be 13.7% and 19.54%, respectively. While 1% gamma alumina was more effective than others in modifying the thermal behavior of paraffine wax, as shown in Fig. 6. The effect of increasing the nanoparticles concentrations on solidification time and thermal behavior under the same conditions is also shown in Figs. 5 and 6. It is inferred that 1% of the two types of alumina were better than 0.5%; however, 1% of Tio_2 insignificantly improved the thermal behavior of PCM compared with 0.5% Tio_2. So, increasing the nanoparticles concentration linearly did not lead to the relative rate of improvement in the thermal behavior of PCM because many factors, such as particles homogenous distribution and slight perturbations in dispersing medium like temperature and PH, play an important role in the enhancement of the nano-PCM solidification time and thermal behavior. Figures 7 and 8 show the nano-PCM temperature distribution with (0.5% and 1% concentrations) at (3 m/s). Figure 7 indicates that paraffine wax with (0.5% alpha and 0.5% gamma) negatively affected the PCM thermal behavior; however, a relative enhancement of nearly 7.69% in solidification time for 0.5% Tio_2 was achieved. Figure 8 indicates that reducing the solidification time of gamma alumina and Tio_2 is (12.3% and 7.69%), respectively, with a mass fraction of 1%. Alpha alumina with a 1% mass fraction provided the most negative results compared to other nano-PCMs at the same velocity. At 5 m/s, all the nanoparticles concentrations showed a negative effect, except 1% Tio_2, as shown in Figs. 9 and 10, due to the repeated thermal cycles, which may lead to agglomeration of particles and change in the behavior of nanomaterials, since thermal cycles may affect the nanoparticles dispersion quality within PCM. So, the ability of nanoparticles to enhance the thermal behavior of PCM and maintain its thermal properties after repeated thermal cycles is crucial. In general, the methods used to determine the state of agglomeration are the same techniques used to measure the size of primary particles, so the AFM test was made for one sample at 1% alumina, as shown in Fig. 11. It is evident from Fig. 11 that the size of the nanoparticles within PCM is larger than primary particles due to a high tendency of nanoparticles for adhesion. Also, a SEM test was performed for 0.5% Tio_2 to determine the agglomeration state, as shown in Fig. 12.

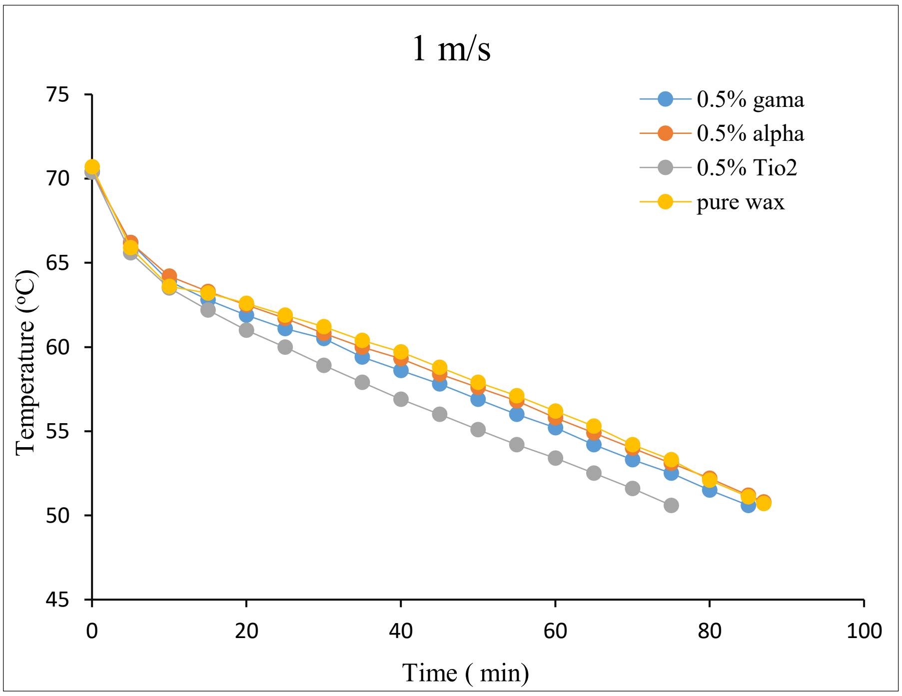

Fig. 5 The Experimental Effect of 0.5% Concentrations on the Thermal Behavior of PCM at 1 m/s.

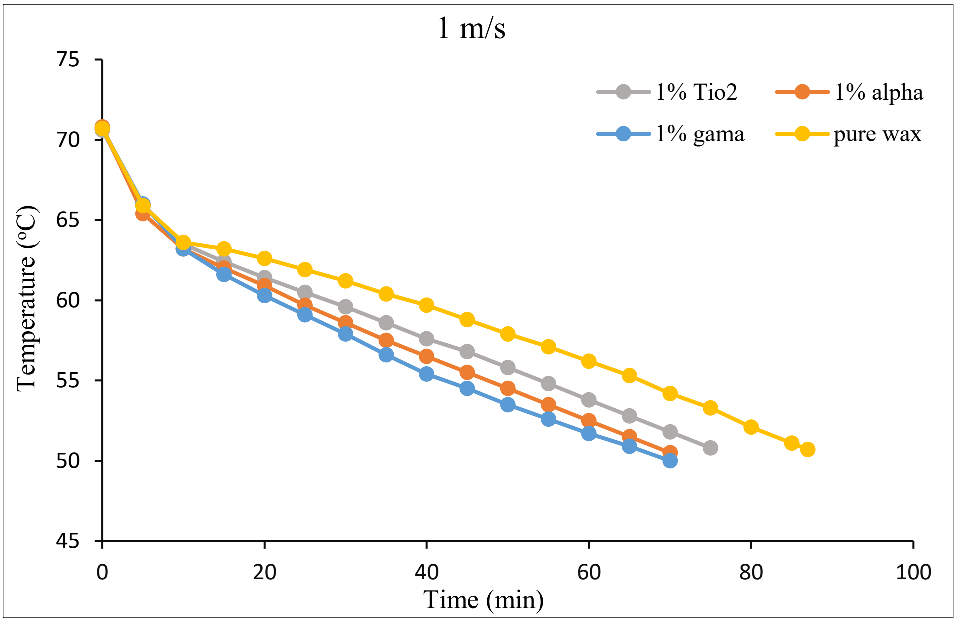

Fig. 6 The Experimental Effect of 1% Concentrations on the Thermal Behavior of PCM at 1 m/s.

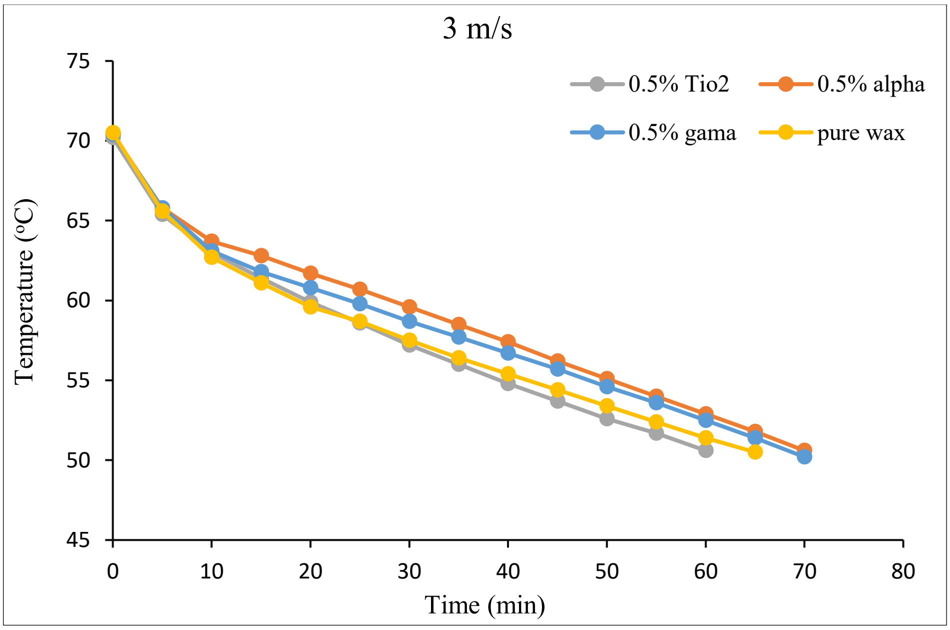

Fig. 7 The Experimental Effect of 0.5 % Concentrations on the Thermal Behavior of PCM at 3 m/s.

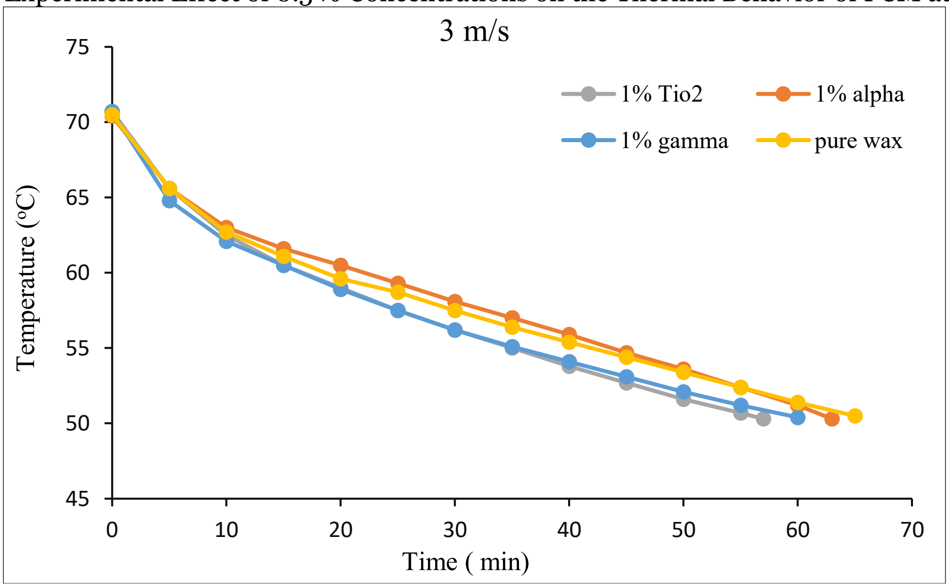

Fig. 8 The Experimental Effect of 1% Concentrations on the Thermal Behavior of PCM at 3 m/s.

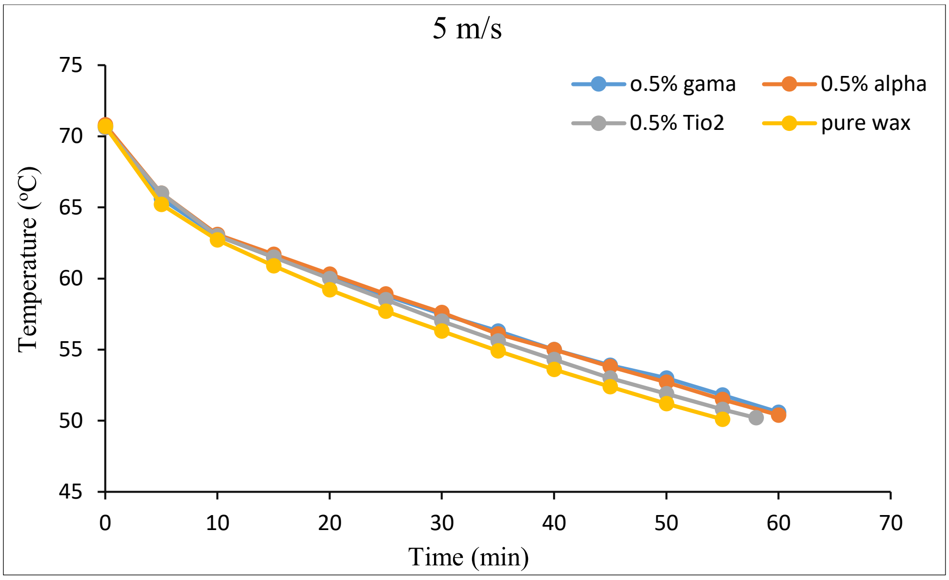

Fig. 9 The Experimental Effect of 0.5% Concentrations on the Thermal Behavior of PCM at 5 m/s.

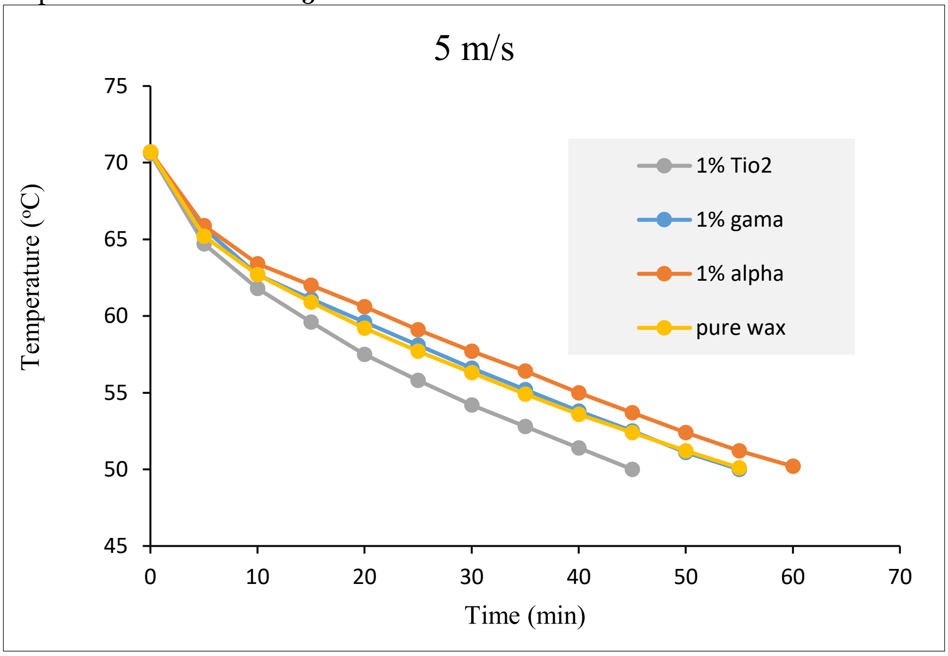

Fig. 10 The Experimental Effect of 1% Concentrations on the Thermal Behavior of PCM at 5 m/s.

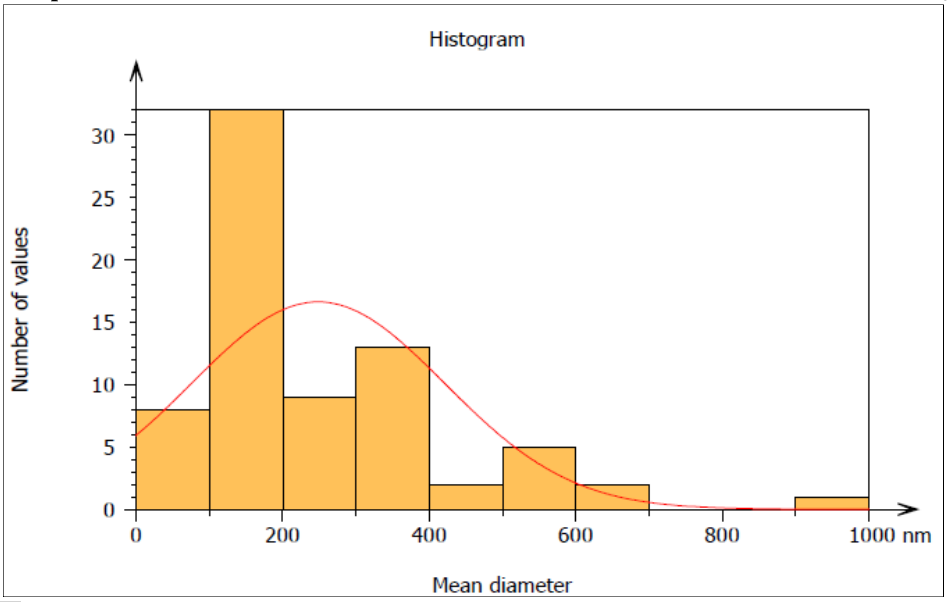

Fig. 11 AFM Test to Determine the State of Agglomeration of Nanoparticles at 1% Alumina.

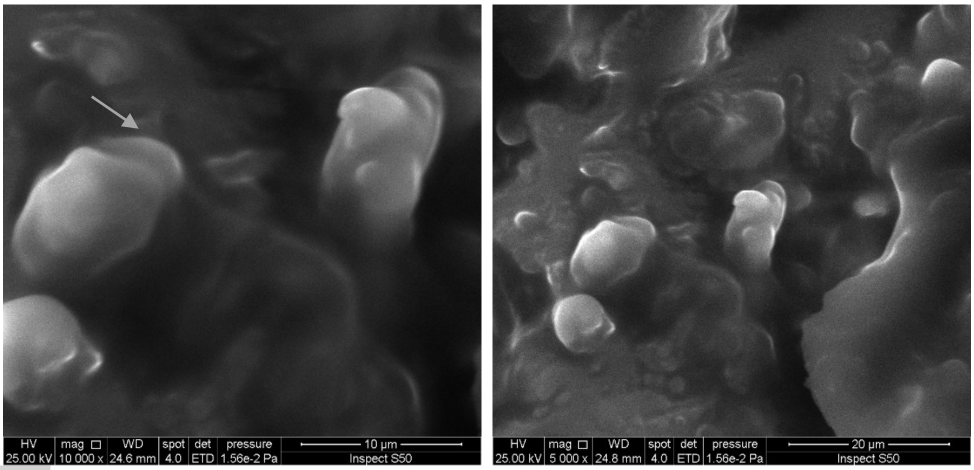

Fig. 12 SEM Test to Determine the State of Agglomeration of Nanoparticles at 0.5% TiO_2.

The primary particles had a high surface-to-volume ratio compared to agglomerated particles. Since most interactions occur at the surface, substances with a high surface-to-volume ratio are expected to have high chemical reactivity compared to those with a low surface-to-volume ratio. Therefore, a high surface-to-volume ratio increases the ability of particles to enhance the heat transfer process. It can be concluded from this paragraph that nanomaterial additions can effectively improve PCM thermal conductivity and enhance its thermal performance; however, nano-composites that have a high nanoparticles concentration with high thermal conductivity do not guarantee the best performance of PCM. Many factors, such as concentration, mixing method, nanoparticles shape, surface charge, and surface chemistry (Chemical Composition of Outermost Layers of Nanomaterials), affect the stability and homogeneity of nanoparticles within PCM, which have a major role in the nano-PCM thermal performance. All these factors require a multidisciplinary approach to determine the nanomaterials' behavior in dispersing medium.

4.2.The Effect of Nanoparticles on Thermophysical Properties

Enhancing the thermal conductivity of phase change material is the primary purpose for adding nanoparticles. Figure 13 shows the thermal conductivity results of pure paraffin wax and nano-PCM. The results showed that the thermal conductivity of all nano-PCM samples was higher than pure PCM, and it indicated that the thermal conductivity increased nonlinearly with the nanoparticles concentration since it depends on the degree of nanoparticles dispersion in the base material and the actual nanoparticle content of the sample. So, the high value of nano-PCM thermal conductivity does not represent the best nano-PCM thermal behavior improvement because it depends on many factors, as explained earlier. The nano-PCM thermal conductivity enhancement compared to pure wax is displayed in Fig. 14, which shows that the largest improvement (56.80%) is obtained at 1% TiO_2 and the minimum improvement of (2.94%) at a mass fraction of 1% gamma.

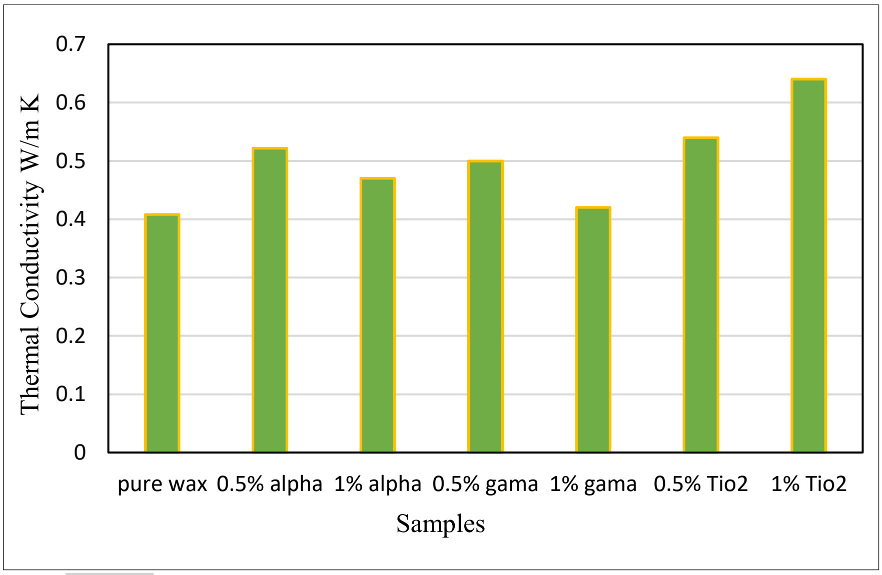

Fig. 13 Thermal Conductivity of Nano-PCM and Paraffine Wax.

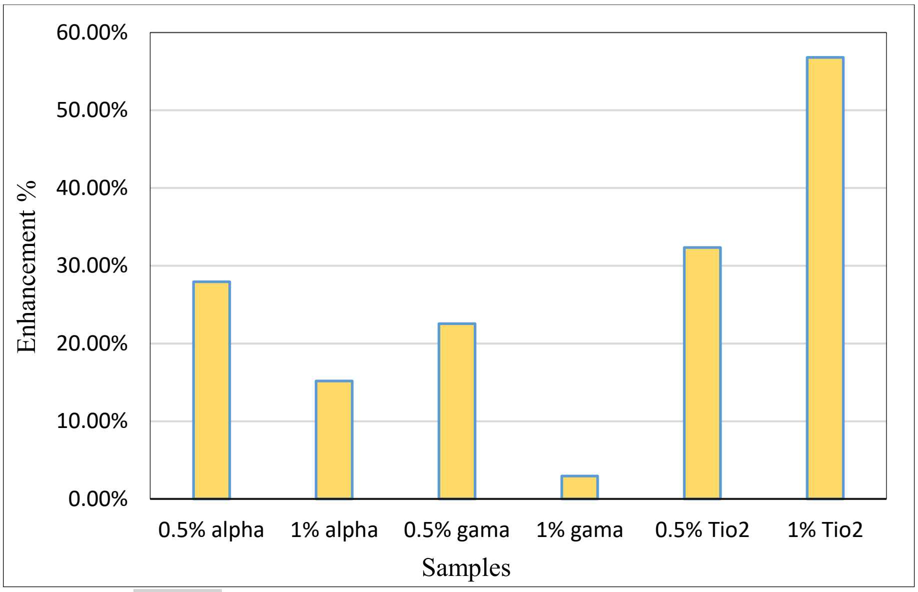

Fig. 14 The Viscosity of Nano-PCM and Paraffine Wax.

The most nano-PCM thermophysical characteristic discussed by researchers, after thermal conductivity, is viscosity. Most of the studies indicated that the nanoparticles inclusion in liquid PCM increased the viscosity due to higher interactions among the nanoparticles, decreasing the particle's sedimentation. So, if the Liquid PCM has a high viscosity, the particles have a lower tendency to move downward. Figure 15 shows how adding nanoparticles to PCM affects viscosity behavior. The results indicated that nano-PCMs with both concentrations have a higher viscosity than pure PCM, except at 1% gamma. Increasing the concentration of alpha particles linearly increased viscosity. Besides, 0.5% alpha and 0.5% gamma have the same effect on the viscosity behavior.

4.3.Behavior of Thermal Power and Nusselt Number of HTF

In Fig. 16, it can be seen how thermal power and HTF speeds are related to pure paraffine and nano-PCM. At the lowest velocity of HTF (1 m/s), the thermal power of all concentrations was almost identical, except at (0.5% TiO_2 and 1% gamma) since the improvement in heat transfer rate at these concentrations was (15.67% and 68.64%), respectively. While, at (3 m/s), the highest heat transfer rate increased by 1% TiO_2 since the improvement in thermal power at this concentration was 25.5%. At (5 m/s), the thermal power at (0.5% concentrations) for all nano-PCM types was almost identical, and at (1% concentrations), an adverse effect was indicated due to the thermal cycle effect on the nanoparticles dispersion quality within PCM, as was concluded in the previous paragraph.

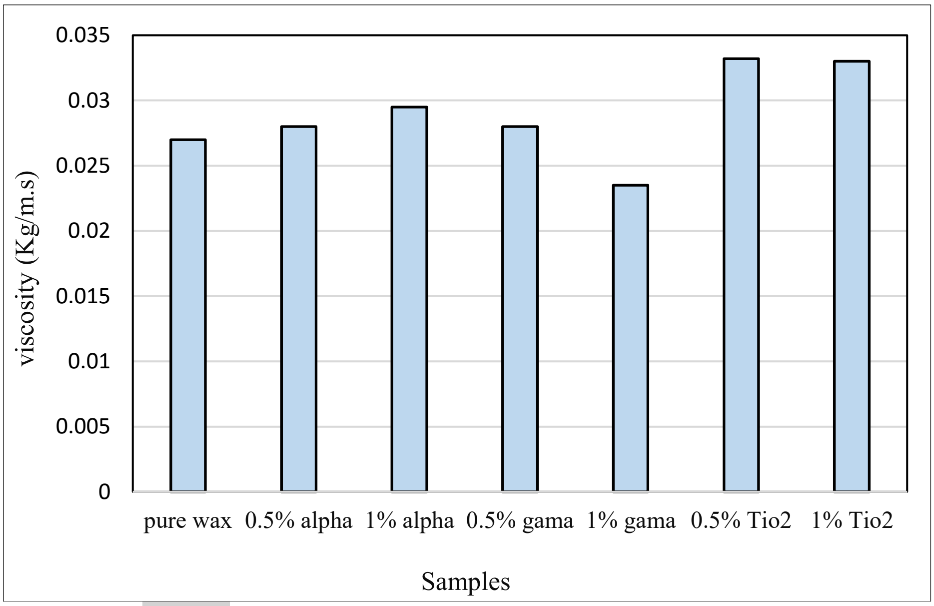

Fig. 15 The Viscosity of Nano-PCM and Paraffine Wax.

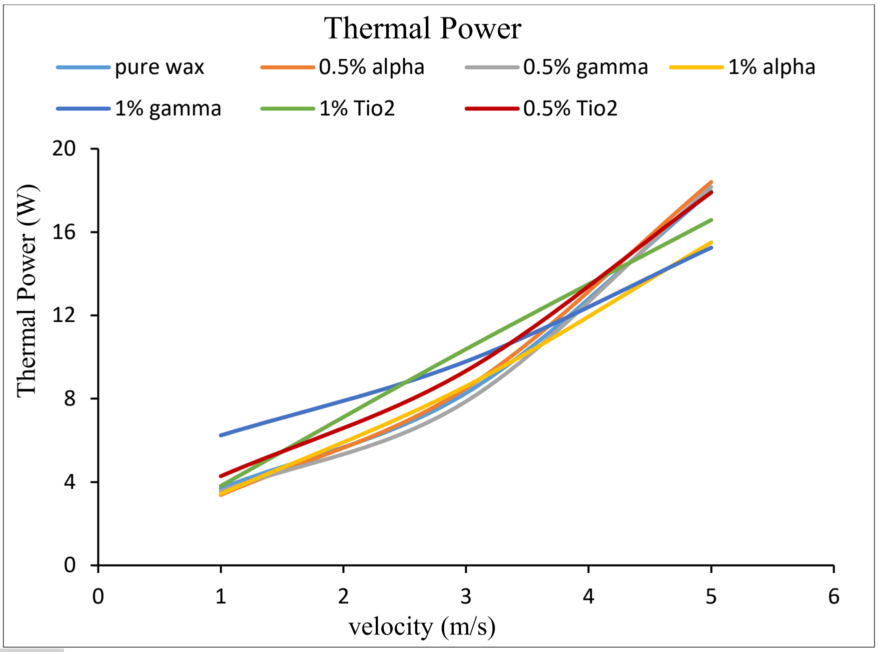

Fig. 16 The Experimental Behavior of Thermal Power for Discharging Process.

Figure 17 shows a Nusselt number value against the speeds of HTF for various nano-PCM mixtures and pure PCM. As in thermal power, the behavior of the Nusselt number for all cases is almost consistent with that of thermal power. The comparison shows that, overall, paraffine with 1% gamma at (1m/s) had the highest value of Nusselt number flow by 0.5% TiO_2 since the improvement was (75.1%) and (13%), respectively. The higher value of the Nuselte number for these two cases indicated that these nanoparticles concentrations influenced the paraffine thermal conductivity and contributed to the enhancement of heat transfer between PCM and HTF since it also depends on the HTF temperature. The results also showed that repeated thermal cycles limited effective Nuselt number because of agglomerate and nanoparticle instability, so adverse effects can be seen at (5 m/s). The temperature distribution behavior in Fig. 6 agrees with cases 1 and 2, which were the results of Sadiq and Mussa [20], as shown in Fig. 18. In addition, the enhancement in the temperature distribution of nano-PCM in the discharging process compared to pure PCM of Fig. 19, which were the results of Abdulateef et al. [21], is similar to the present results, as shown in Fig. 6, qualitatively, not quantitatively, due to the difference in concentration and type of nanoparticles. However, the same behavior was obtained as mentioned above.

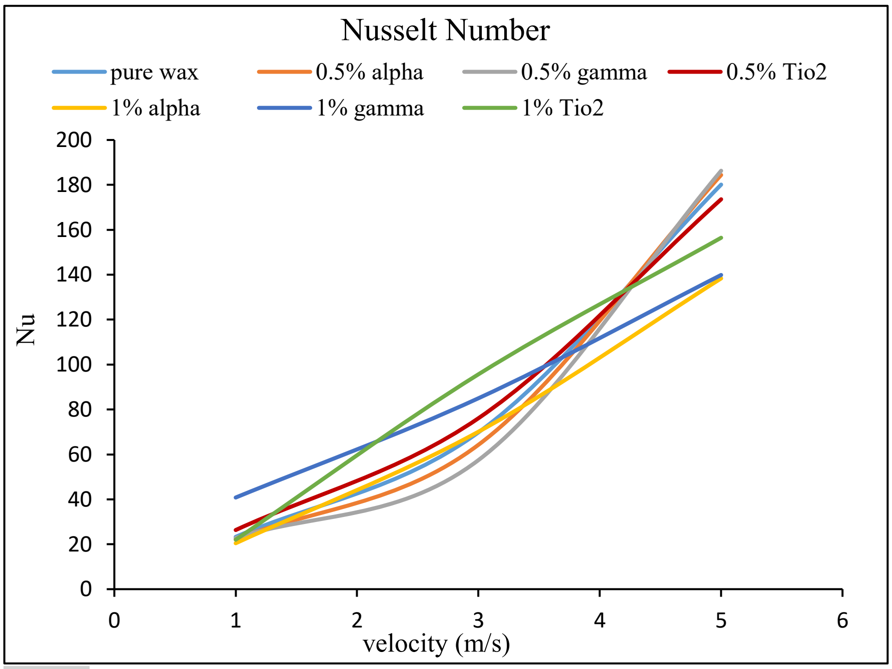

Fig. 17 Experimental Behavior of Nusselt Number for Discharging Process.

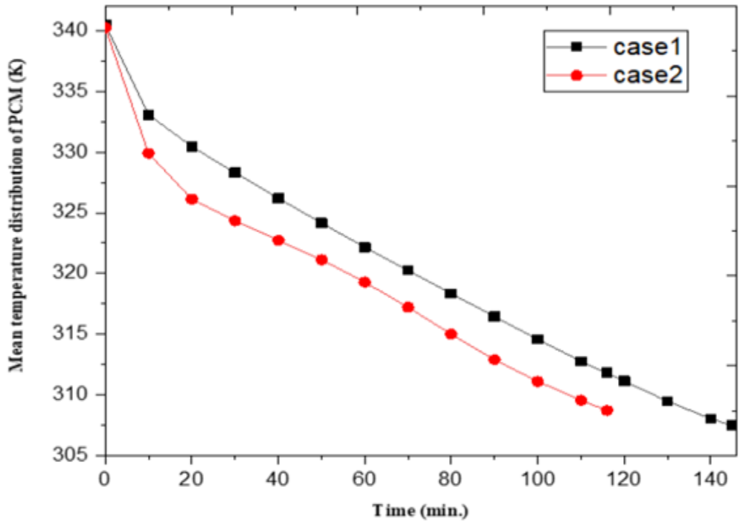

Fig. 18 The Result of the Temperature Distribution Profile of Reference [20].

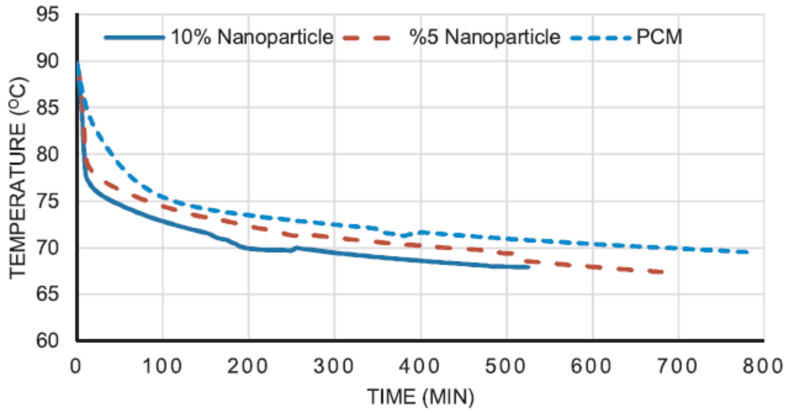

Fig. 19 The Result of the Temperature Distribution Profile of Reference [21].

5.CONCLUSIONS

The influence of Al_2O_3 and TiO_2 nanoparticles on the thermal behavior and thermal properties of paraffin wax was experimentally investigated with concentrations of (0.5% and 1%). The following is the summary of the study conclusions:

- Nano-composites that have a nanoparticle with high thermal conductivity do not guarantee the best performance of PCM. Many factors, such as stability, homogeneity of nanoparticles within PCM, and concentration, have a major role in the thermal performance of nano-PCM. Therefore, at (1 m/s), paraffin mixed with (0.5% TiO_2) was better than paraffin mixed with (0.5% gamma) and (0.5% alpha). At 1% concentration and the same velocity, gamma alumina was more effective than other studied nanoparticles in modifying the paraffine wax thermal behavior.
- Increasing the nanoparticles concentration linearly did not lead to the relative rate of improvement in the thermal behavior of PCM, so (1% Tio2) at the first thermal cycle (1 m/s) insignificantly increased the PCM thermal behavior improvement compared with 0.5% Tio2.
- (1%) gamma was the optimum particle concentration in the paraffin since the improvement in heat transfer rate at these concentrations was (68.64%) at the first thermal cycle.
- The thermal conductivity increased nonlinearly with the nanoparticles concentration since it depends on the nanoparticles dispersion degree in the base material and the actual nanoparticle content of the sample.

ACKNOWLEDGEMENTS

The authors would like to acknowledge the support of the Mechanical Engineering Department at the College of Engineering - University of Baghdad, Iraq, for the present work, which is a part of M.Sc. thesis research for the first author supervised by the second author.

NOMENCLATURE

AFM	Atomic Force Microscope
CTES	Cascade Thermal Energy Storage
FPSC	Flat Plate Solar Collector
HTF	Heat Transfer Fluid
LHES	Latent Heat Energy Storage
LMTD	Log-Mean Temperature Difference
PCM	Phase Change Material
TES	Thermal Energy Storage System

A_c	Cross Section Area (m^2)
A_s	Surface Area (m^2)
C_p	Specific heat (J/kg·K)
D_h	Hydraulic Diameter (m)
ha	Convective Heat Transfer Coefficient (kJ/kg)
K_a	Thermal Conductivity of Air (W/m.°C)
m_{np}	Mass of Nanoparticles (kg)
p	Perimeter (m)
T_{in}	Inlet Air Temperature (°C)
T_{out}	Outlet Air Temperature (°C)
$\dot{m}$	Mass Flow Rate of Air (kg/s)
Greek symbols	
ρ	Density, kg/m^3
μ	Viscosity (Pa. s)
$\emptyset$	Nanoparticles Concentration
Subscripts	
c	Cross Section Area
s	Surface Area
in	Inlet
out	Outlet
np	Nanoparticles

REFERENCES

[1] Chaichan MT, Hussein RM, Jawad AM. **Thermal Conductivity Enhancement of Iraqi Origin Paraffin Wax by Nano-Alumina**. *Al-Khwarizmi Engineering Journal* 2017; **13**(3): 83-90.

[2] Ghalambaz M, Mehryan SAM, Ayoubloo KA, Hajjar A, El Kadri M, Younis O, Hulme-Smith C. **Thermal Energy Storage and Heat Transfer of Nano-Enhanced Phase Change Material (NEPCM) in a Shell and Tube Thermal Energy Storage (TES) Unit with a Partial Layer of Eccentric Copper Foam.** *Molecules* 2021; **26**(5): 1491, (1-20).

[3] Tao YB, Ya-Ling He. **A Review of Phase Change Material and Performance Enhancement Method for Latent Heat Storage System**. *Renewable Sustainable Energy Reviews* 2018; **93**: 245-259.

[4] Buonomo B, Di Pasqua A, Ercole D, Manca O. **Numerical Study of Latent Heat Thermal Energy Storage Enhancement by Nano-PCM in Aluminum Foam**. *Inventions* 2018; **3**(4):76, (1-11).

[5] Valan AA, Sasmito AP, Mujumdar AS. **Numerical Performance Study of Paraffin Wax Dispersed with Alumina in a Concentric Pipe Latent Heat Storage System**. *Thermal Science* 2013; **17**(2): 419-430.

[6] Harikrishnan S, Deenadhayalan M, Kalaiselvam S. **Experimental Investigation of Solidification and Melting Characteristics of Composite PCM for Building Heating Application**. *Energy Conversion Management* 2014; **86**: 864-872.

[7] Sadiq HH, Mussa MA. **Numerical Study of Thermal Conductivity Effect on the Performance of Thermal Energy Storage**. *Journal of Engineering* 2022; **28**(10): 57-77.

[8] Altaee TM. **Improvement of Diesel Fuel Engine Performance by Nanoparticles Additives**. *Journal of Engineering* 2022; **28**(4): 77-90.

[9] Al-Ali D, Kamoona GMI. **Effectiveness of Nanomaterial in the Roof of the Building to Achieve Energy Conservation for Indoor Environment of the Building**. *Journal of Engineering* 2021; **27**(2): 126-148.

[10] Sarsam WS, Kazi SN, Badarudin A. **Thermal Performance of a Flat-Plate Solar Collector Using Aqueous Colloidal Dispersions of Multi-Walled Carbon Nanotubes with Different Outside Diameters.** *Experimental Heat Transfer* 2022; **35**(3): 258-281.

[11] Hussein AK. **Applications of Nanotechnology in Renewable Energies—A Comprehensive Overview and Understanding**. *Renewable Sustainable Energy Reviews* 2015; **42**: 460-476.

[12] Arasu A, Sasmito A, Mujumdar A. **Thermal Performance Enhancement of Paraffin Wax with Al_2O_3 and CuO Nanoparticles–A Numerical Study**. *Frontiers in Heat and Mass Transfer* 2012; **2**(4): 1-7.

[13] Mahdi JM, Nsofor EC. **Solidification of a PCM with Nanoparticles in Triplex-Tube Thermal Energy Storage System**. *Applied Thermal Engineering* 2016; **108**: 596–604.

[14] Chaichan MT, Kamel SH, Al-Ajeely ANM. **Thermal Conductivity Enhancement by Using Nano-Material in Phase Change Material for Latent Heat Thermal Energy Storage Systems**. *Saussurea* 2015; **5**(6): 48-55.

[15] Pradeep N, Paramasivam K, Rajesh T, Purusothamanan VS, Iyahraja S. **Silver Nanoparticles for Enhanced Thermal Energy Storage of Phase Change Materials** *Materials Today: Proceedings* 2021; **45**: 607-611.

[16] Teng TP, Yu CC. **Characteristics of Phase-Change Materials Containing Oxide Nano-Additives for Thermal Storage**. *Nanoscale Research Letters* 2012; **7**: 1-10.

[17] Venkateshwar K, Joshy N, Simha H, Mahmud S. **Quantifying the Nanoparticles Concentration in Nano-PCM**. *Journal of Nanoparticle Research* 2019; **21**: 1-10.

[18] Li D, Wang Z, Wu Y, Liu C, Arıcı M. **Experimental Investigation on**

Thermal Properties of Al2O3 Nanoparticles Dispersed Paraffin for Thermal Energy Storage Applications. *Energy Sources, Part A: Recovery, Utilization, and Environmental Effects* 2021: **46**(1): 8190-8200.

[19] Hasan HA, Hussain IY. **Experimental Investigation of Thermal Performance Enhancement of Cascade Thermal Energy Storage System by Using Metal Foam**. *International Journal of Mechanical Engineering and Technology* 2018; **9**(9): 1537-1549.

[20] Sadiq HH, Mussa MA. **Experimental Study of Thermal Conductivity Effect on the Performance of Thermal Energy Storage**. *Jordan Journal of Mechanical & Industrial Engineering* 2022; **16**(4): 557-566.

[21] Abdulateef AM, Abdulateef J, Al-Abidi AA, Sopian K, Mat S, Mahdi MS. **A Combination of Fins-Nanoparticle for Enhancing the Discharging of Phase-Change Material Used for Liquid Desiccant Air Conditioning Unite**. *Journal of Energy Storage* 2019; **24**: 100784.

[22] Khalaf SM, Mohammed AA, Mohammed QJ. **An Experimental Investigation on Heat Transfer Enhancement in an Annulus with Rotating Outer Cylinder Using Nano Fluids.** *Tikrit Journal of Engineering Sciences* 2022; **29**(2): 51-60.

[23] Chaichan MT, Kazem HA. **Single Slope Solar Distillator Productivity Improvement Using Phase Change Material and Al_2O_3 Nanoparticle**. *Solar Energy* 2018; **164**: 370-381.

[24] Cengel Y. **Heat and Mass Transfer - A Practical Approach**. 3rd ed., New York, NY, USA: Mc Graw Hill; 2007.

[25] Bergman T, Lavine A, Incropera F, Dewitt D. **Fundamentals of Heat and Mass Transfer**. 7th ed., USA: John Wiley & Sons; 2011.

[26] Holman JP. **Experimental Methods for Engineers**. 8th ed., Americas, New York, NY: McGraw-Hill Higher Education; 2011.